THE JOURNAL OF COMPARATIVE NEUROLOGY 417:32–48 (2000)

Theta Ganglion Cell Type of Cat Retina

T. ISAYAMA, D.M. BERSON*, AND M. PU
Department of Neuroscience, Brown University, Providence, Rhode Island 02912

ABSTRACT

We define a new bistratified ganglion cell type of cat retina using intracellular staining in vitro. The theta cell has a small soma, slender axon, and delicate, highly branched dendritic arbor. Dendritic fields are intermediate in size among cat ganglion cells, with diameters typically two to three times those of beta cells. Fields increase in size with distance from the area centralis, ranging in diameter from 70 to 150 μm centrally to a maximum of 700 μm in the periphery. Theta cells have markedly smaller dendritic fields within the nasal visual streak than above or below it and smaller fields nasally than temporally. Dendritic arbors are narrowly bistratified. The outer arbor lies in the lower part of sublamina *a* (OFF sublayer) of the inner plexiform layer where it costratifies with the dendrites of OFF alpha cells. The inner arbor occupies the upper part of sublamina *b* (ON sublayer), where it costratifies with ON alpha dendrites. The outer and inner arbors are composed of many relatively short segments and are densely interconnected by branches that traverse the *a*/*b* sublaminar border. Experiments combining retrograde labeling with intracellular staining indicate that theta cells project to the superior colliculus and to two components of the dorsal lateral geniculate nucleus (the C laminae and medial interlaminar nucleus). Theta cells project contralaterally from the nasal retina and ipsilaterally from the temporal retina. They apparently correspond to a sluggish transient or phasic W-cell with an ON-OFF receptive field center. J. Comp. Neurol. 417:32–48, 2000.

Indexing terms: W-cell; sluggish; visual streak; superior colliculus; lateral geniculate nucleus; medial interlaminar nucleus

Fundamental to vertebrate vision are the different types of retinal ganglion cells and their projections to different regions of the brain. These cell types can be objectively distinguished from one another by the absence of intermediate forms (Boycott and Wässle, 1974; Rowe and Stone, 1977; Rodieck and Brening, 1983; Stone, 1983; Rodieck, 1998). To date, eight ganglion cell types in cat retina have been formally classified in this way: alpha-ON, alpha-OFF, beta-ON, beta-OFF, delta (monoamine-accumulating), epsilon, zeta, and eta cells (Boycott and Wässle, 1974; Wässle et al., 1975, 1981; Leventhal et al., 1980; Dacey, 1989; Wässle and Boycott, 1991; Pu et al., 1994; Berson et al., 1998, 1999).

All these types are unistratified. With one exception, they ramify exclusively in either sublamina *a* (the OFF sublayer) or in sublamina *b* (the ON sublayer) of the inner plexiform layer. The exceptional type, the zeta cell, stratifies narrowly at the border between these sublaminae (Berson et al., 1998). However, various ganglion cells ramifying in both sublamina *a* and *b* have been encountered in cat retina. Some of these are diffusely stratified and others are narrowly bistratified (Kolb et al., 1981; Famiglietti, 1987). These cells are of interest because they may correspond to physiological types receiving input from both the ON and OFF channels. Here we define a new bistratified ganglion cell type in cat retina, a type termed the theta cell.

MATERIALS AND METHODS

Methods will be only briefly summarized, as they have been described in detail previously (Pu and Berson, 1992; Pu et al., 1994; Berson et al., 1998, 1999). The term "delta," introduced by Boycott and Wässle (1974), is used here to refer specifically to the ganglion cell type known to accumulate monoamines (Wässle et al., 1987; Dacey, 1989).

Grant sponsor: National Eye Institute; Grant number: PHS 5 R01 EY06108.

M. Pu's current address is: Department of Neurobiology and Anatomy, University of Utah College of Medicine, Salt Lake City, UT 84132.

*Correspondence to: David M. Berson, Department of Neuroscience, Box 1953, Brown University, Providence, RI 02912.
E-mail: David_Berson@Brown.edu.

Received 15 June 1999; Revised 8 October 1999; Accepted 13 October 1999

Dye injection and histochemistry

Ganglion cells were stained by visually guided intracellular injection of Lucifer Yellow and either biocytin or neurobiotin in the living retina in vitro. Methods conformed with NIH guidelines and were approved by Brown University's Institutional Animal Care and Use Committee. Cats were deeply anesthetized with Nembutal (35 mg/kg ip) and, following eye removal, killed by Nembutal overdose with or without vascular perfusion with 4% buffered paraformaldehyde (pH 7.4). Retinas were isolated and superfused at room temperature with oxygenated Ames' medium (Sigma).

In about half of the experiments (30 retinas from 21 cats), we targeted ganglion cells stained supravitally with acridine orange (see Pu et al., 1994 for details). In some of these experiments, we injected alpha ganglion cells lying near stained theta cells to serve as benchmarks in the analysis of dendritic stratification. In the remaining experiments (32 retinas from 19 cats), we injected cells labeled by retrograde transport of fluorescent microspheres deposited in the superior colliculus or various divisions of the lateral geniculate nucleus. The location of these deposits and the methods used to produce them are detailed elsewhere (Pu and Berson, 1991, 1992; Pu et al., 1994; Stein et al., 1996; Berson et al., 1998, 1999).

Alpha, beta, delta, epsilon, zeta, and eta cells stained in these experiments were used for various morphometric comparisons. Details on the distribution of these cells among individual retinas are available elsewhere (Table 1 of Berson et al., 1999). Comparisons of soma size are based on a sample of 100 delta cells (19.2 $\pm$ 2.9 μm); 22 epsilon cells (19.2 $\pm$ 3.1 μm); 154 zeta cells (mean soma size $\pm$ SD 16.0 μm $\pm$ 1.7 μm); and 112 eta cells (15.6 $\pm$ 2.3 μm).

Retinas were fixed and processed immunohistochemically as previously described (Pu and Berson, 1992; Berson et al., 1998). Some retinas were dehydrated and cleared, and others were coverslipped with 60% buffered glycerol (pH 7.4) without prior dehydration or clearing. Horizontal shrinkage was negligible with either method (see Pu et al., 1994), and shrinkage in depth was minimal with the glycerol method, which was used for all quantitative analyses of stratification. Depth measurements with dry objectives were corrected according to Snell's law (Berson et al., 1998).

Microscopic analysis

The positions of the area centralis and visual streak were determined from vascular patterns and the densities of ganglion cells, visible from nonspecific histochemical labeling. Dendritic field measurements were made only in cells judged to be fully stained. Diameters of dendritic fields and of somata were taken as the mean of the maximal and minimal diameters as measured with an eyepiece graticule. This method yields results very similar to those obtained by determining the area of a convex polygon minimally encompassing the dendritic profile and was preferred for its efficiency (Berson et al., 1999).

A general impression of the depth of dendritic stratification could be obtained by through-focus analysis. Benchmarks for the limits of the inner plexiform layer (IPL) included somata of ganglion and amacrine cells and dark granules marking the outer limit of the IPL (Berson et al., 1998, 1999). Using these reference points, it was almost always possible using through-focus analysis to determine with confidence whether a stained alpha or beta cell belonged to the *a* (OFF) or *b* (ON) subtype. For many of the alpha cells, this judgment could be confirmed because of overlap with another intracellularly stained alpha cell of opposite type. Selected cells were reconstructed in three dimensions using a digital morphometry system (Neurolucida; MicroBrightfield, Colchester, VT).

Photomicrographs in this report were shot with Kodak T-Max 100 film. Negatives were digitally scanned (Nikon Coolscan) and then processed and printed using Photoshop software (Version 4.0; Adobe). Only globally applied filters were used on each image.

RESULTS

Theta cells had densely branched, highly overlapping dendritic fields that were intermediate in size among cat ganglion cells. They had small somata and thin axons. The camera lucida drawings of Figure 1 illustrate the form of representative theta cells at various retinal locations. The photomicrographs of Figure 2 display some of the morphological features of these cells.

Somatic and axonal morphology

Somata were ovoid or round and ranged in diameter from 10 to 21 μm (mean $\pm$ SD, 15.3 $\pm$ 2.0 μm; n = 116). Somatic size varied little with retinal eccentricity (Fig. 3A) or distance from the visual streak (not shown) although cells in the central 1 mm tended to be slightly smaller on average than those in the periphery. Theta cells had among the smallest cell bodies of all cat ganglion cell types. Their somata were much smaller than any alpha cell we have stained by the same method. They were also typically smaller than beta cells as well (Fig. $2D_1$ and E_1), although there was overlap between the populations (Fig. 3B). Theta cell somas were significantly smaller on average than those of delta, epsilon, and zeta cells ($P < 0.005$; two-tailed t-test, inhomogeneous variances) but were statistically indistinguishable from those of eta cells ($P > 0.05$; two-tailed t-test, homogeneous variances).

Axons of theta cells were typically slender, apparently less than 1 μm in diameter, and comparable in caliber to those of cat zeta and eta cells (Berson et al., 1998, 1999). They were substantially thinner than the axons of beta cells (Fig. $2D_2$ and E_2) and slightly thinner on average than those of epsilon and delta cells stained by this method. Theta cell axons nearly always emerged from the soma, but in a few cells arose from a stout primary dendrite (e.g., Fig. 1, cell O). Some had a few short branches of the sort typically associated with zeta cell axons (Berson et al., 1998). In one unusual theta cell, the axon bifurcated 300 μm from the soma, and both daughter branches could be traced >4 mm toward the optic nerve head.

Dendritic morphology

Theta cells had some of the most densely branched and highly overlapping dendritic arbors we have observed among cat ganglion cells. Typically the arbors arose from two to four primary dendrites. Most dendrites were very slender, much thinner than the dendrites of alpha, beta, and epsilon cells (Fig. 2A–C; see Fig. 10), although dendrites of low branch order were of moderate thickness, especially in the peripheral retina. Dendrites were generally fairly smooth, although some exhibited varicosities or short spines. Dendritic profiles were "tufted" in that branching was abundant in the periphery of the field (Ramón-Moliner, 1962; Famiglietti, 1992b). The slender preterminal and terminal processes bore no consistent

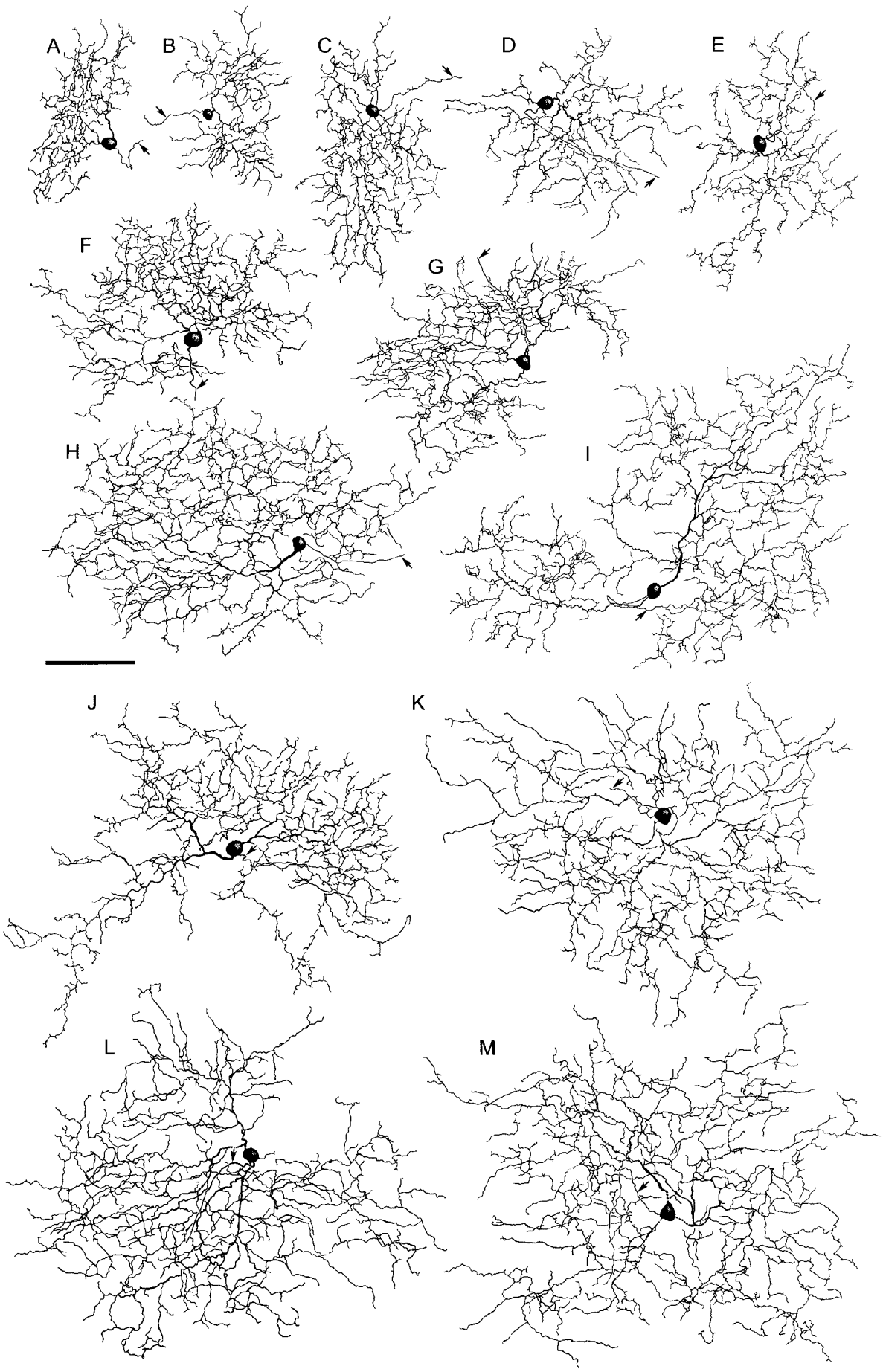

Figure 1

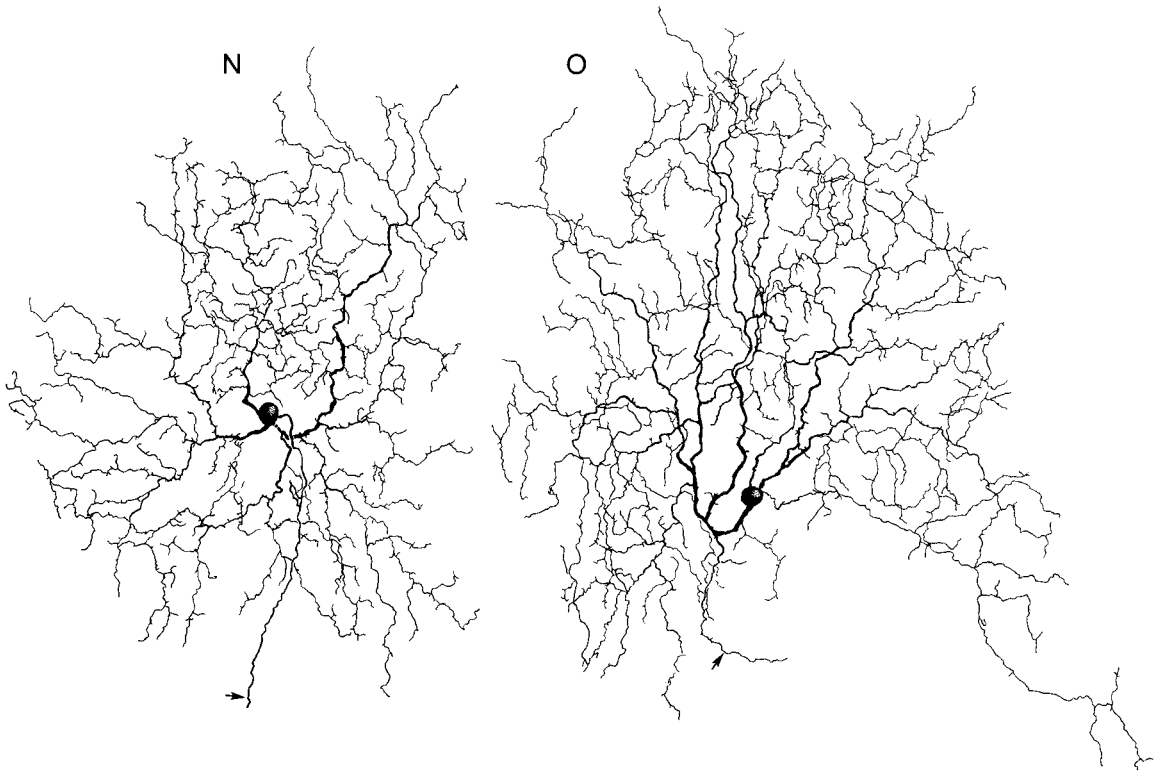

Fig. 1. **A–O:** Camera lucida drawings of stained theta cells in retinal wholemounts. All drawings are at the same scale. Arrows indicate axons. Photomicrographs of cell F appear in Figure 2B, F, and G; photos of cell I appear in Figure 2A, H, and I; and photos of cell O appear in Figure 2C and D. Eccentricities (e) and distances from the visual streak axis (s) in millimeters as follows: A: e = −0.3, s = +0.1; B: e = −0.5, s = +0.4; C: e = −0.5, s = −0.5; D: e = +4.8, s = −0.3; E: e = +8.6, s = +0.7; F: e = +1.5, s = −1.3; G: e = −0.4, s = +0.3; H: e = −1.8, s = +1.8; I: e = −3.5, s = −2.4.; J: e = +5.0, s = −1.5; K: e = +8.0, s = +6.0; L: e = −1.6, s = +1.4; M: e = +5.6, s = −3.9; N: e = +8.7, s = −5.2; O: e = +10.6, s = −7.6. Negative eccentricities denote locations in temporal hemiretina, and negative streak distances indicate locations in inferior hemiretina. Cells G and L were labeled by retrograde transport from the ipsilateral superior colliculus and cell J from the contralateral medial interlaminar nucleus of the lateral geniculate. Scale bar = 100 μm.

orientation with respect to the soma. Many took tortuous courses or doubled back toward the cell body. Dendritic overlap was a prominent feature in many parts of the field, although not all. The waviness, bushiness, and mutual overlap among the processes lent most cells a chaotic, tangled aspect. Dendritic fields were generally compact, with well-defined perimeters, although isolated branches sometimes protruded from the main arbor (e.g., Fig. 1O), and there were often patchy variations in branching density within the field. Field envelopes were typically circular, although some were moderately ellipsoid (Fig. 1A,C,E) or irregularly shaped (Fig. 1I,J). Most somata were centered within the arbor's perimeter, but some were eccentric (e.g., Fig. 1A,B,D,F).

Dendritic field size: Topography and comparison with other ganglion cell types

Dendritic field size ranged from 80 to 700 μm. Variations in size were analyzed with respect to retinal eccentricity (radial distance from the center of the area centralis) and distance superior or inferior to the visual streak, a horizontal band of elevated ganglion cell density that passes through the area centralis (Hughes, 1977). Field size was related to eccentricity (Fig. 4A). Only cells with small fields (<310 μm in diameter) were observed in the central retina (<1 mm eccentricity), whereas cells with the largest fields (>460 μm in diameter) invariably lay in the retinal periphery (eccentricities >2 mm temporally and >4 mm nasally).

In the nasal periphery, field size varied widely, and this variation was systematically related to the position of cells relative to the visual streak. Cells lying nearest the streak (Fig. 4A, filled diamonds) had the smallest dendritic fields at every eccentricity whereas those farthest from the streak (open circles) had the largest fields. This relationship is evident among the cells shown in Figure 1. For example, Cells E, K, and N all lay in the nasal retina roughly equidistant from the area centralis (8–9 mm), but Cell E lay much closer to the visual streak than did Cells K and N and had a much smaller field. Figure 4B, which plots field size as a function of distance from the visual streak axis, confirms the correlation between these variables in the nasal retina. Among nasal cells overall, streak distance accounted for more than three times as much of the variance in field size ($r^2 = 0.61$), as did eccentricity ($r^2 = 0.17$). Because eccentricity and streak distance are not independent measures, the substantial correlation between field size and distance from the visual streak (Fig. 4B) ensures at least a weak relationship between field size and eccentricity (Fig. 4A; see Berson et al., 1998, for elaboration). However, eccentricity per se clearly exerts an independent influence. For example, among cells lying within 0.5 mm of the streak (filled diamonds in Fig. 4A), field size increased with eccentricity. In the central retina, eccentricity appeared to be a better predictor of field size than did streak distance.

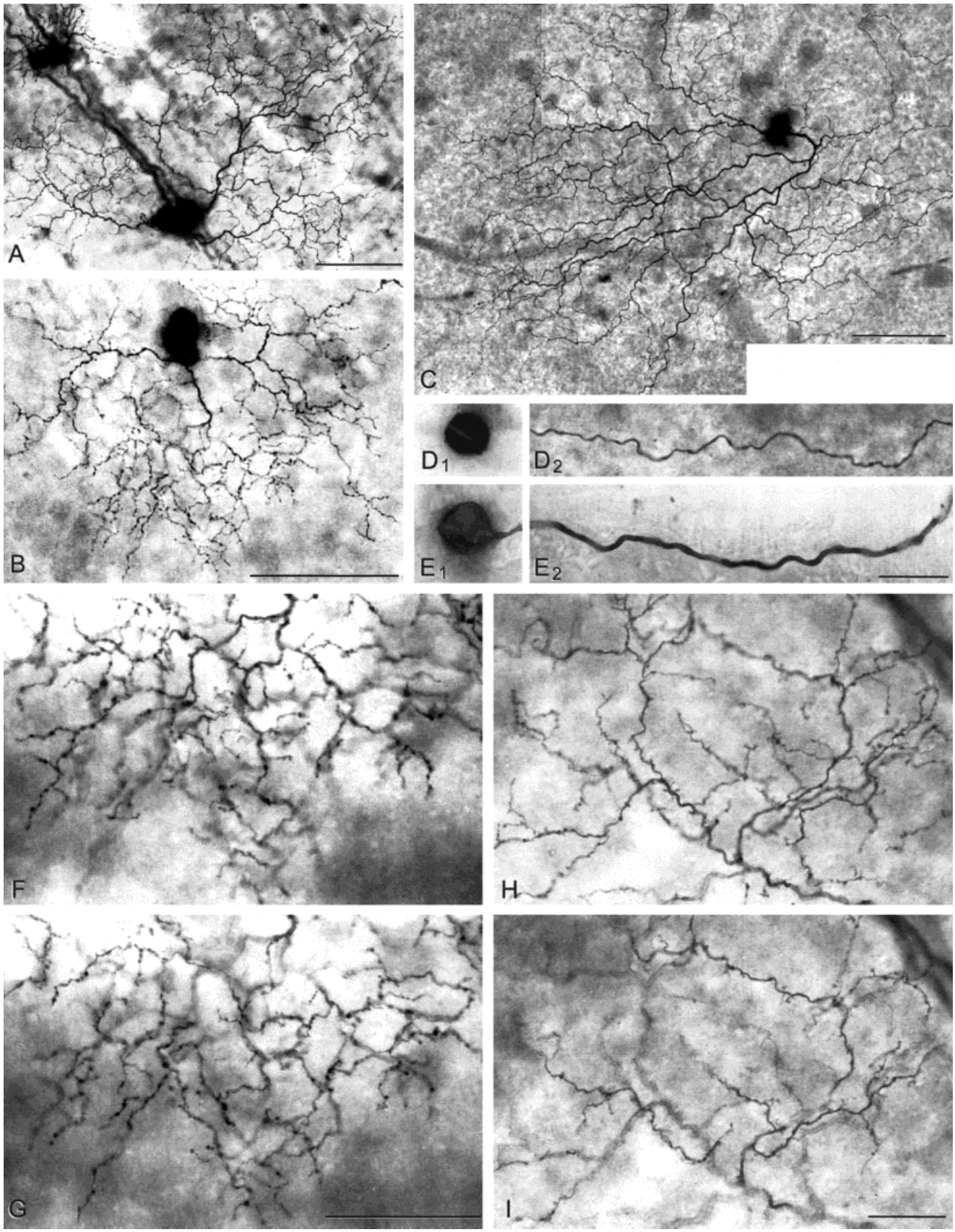

Figure 2

In the temporal hemiretina, dendritic fields were substantially larger than they were nasally (Fig. 5; see also Fig. 4A,B), and eccentricity was the main topographic determinant of field size. The dispersion of field sizes in the periphery was more modest temporally than nasally and was essentially unrelated to position relative to the visual streak (cf. Fig. 4A,B). What little relationship there was in the temporal retina between field size and streak distance (Fig. 4B) appeared largely attributable to the fact that cells far from the streak are also, by definition, far from the area centralis. There were no apparent differences in field size between superior and inferior retina.

These topographic variations in dendritic field size presumably reflect regional differences in the spatial density of theta cells. Figure 6 shows a plot of these densities obtained by assuming that the dendritic field areas of theta cells are everywhere inversely proportional to their density, as is true for other ganglion cell types (Peichl and Wässle, 1979; Wässle et al., 1981; Dann et al., 1988; Dacey, 1989, 1993b; Vaney, 1994; Stein et al., 1996). More specifically, we assumed that theta cells completely tile the retina with minimum overlap, that is, that their coverage factor (dendritic field area × cell density) is 1 (Berson et al., 1998). Density estimates ranged from 202 cells/mm^2 in the central retina to 3 cells/mm^2 in the far nasal periphery. This analysis may underestimate theta cell density. Upward revision of the coverage constant from the lower-bound estimate used would yield proportional increases in the density estimates. However, the distribution would be unchanged in form and must therefore resemble the actual theta cell distribution provided coverage is topographically invariant, as we have assumed. The isodensity contours are distinctly ellipsoid in the nasal hemiretina, with long axes nearly horizontal, indicating a pronounced concentration of theta cells in the nasal visual streak. This tendency is much stronger than observed for the eta cell (Fig. 6B) or the delta cell (Dacey, 1989) but is comparable to that exhibited by the zeta cell (Fig. 6C), which, among established cat ganglion cell types, is the most strongly concentrated in the streak (Berson et al., 1998).

To assess how well the distribution of Figure 6A encapsulates the topographic variations in theta cell field size, we employed a transform of retinal position termed equivalent eccentricity that compensates for asymmetric cell distributions by bringing together cells from all regions of comparable cell density (Watanabe and Rodieck, 1989). The equivalent eccentricity of a cell is defined as the distance from the area centralis to that point along a standard centrifugal path at which the ganglion cell density matches the density near the cell. Thus, all cells that lie on the same isodensity line have the same equivalent eccentricity despite differences in their distances from the area centralis. Figure 6D shows that there is much less scatter when dendritic field size is plotted as a function of equivalent eccentricity (dots) than when plotted as a function of eccentricity itself (open triangles). This suggests that the map of Figure 6A accounts effectively for topographic variations in theta cell field size and, presumably, in theta cell density.

Figure 7 compares dendritic field sizes of theta cells with those of other types of cat ganglion cells. Theta cell fields (filled diamonds) were intermediate in size between those of alpha cells (open circles) and beta cells (dots), with relatively little overlap among the three populations (Fig. 7A). Field diameters were typically two to three times larger for theta cells than for beta cells and about a third smaller for theta cells than for alpha cells. Most of the apparent overlap between theta and beta cells in the nasal periphery (Fig. 7A) occurs between the relatively small theta cells of the visual streak and the relatively large

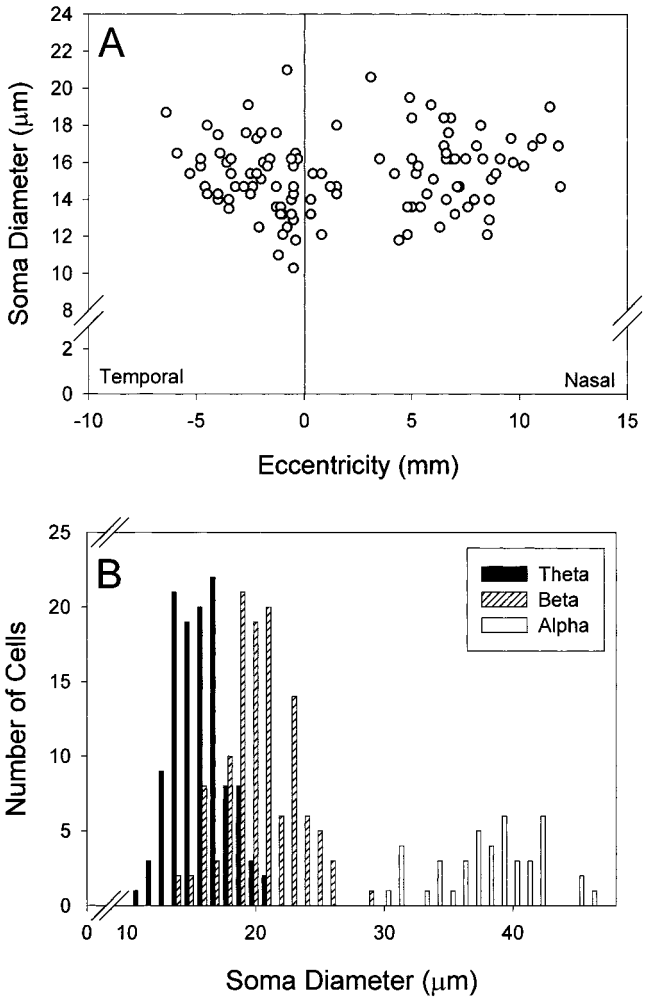

Fig. 3. Soma diameters of theta cells. **A:** Scatterplot of soma diameter as a function of eccentricity. **B:** Histogram comparing soma diameters of theta cells (black bars) with those of beta cells (hatched bars) and alpha cells (white bars) stained by identical methods.

Fig. 2. Photomicrographs illustrating morphologic details of intracellularly stained theta cells. **A–C:** Three theta cells at low magnification. **D**: Soma (D_1) and axon (D_2) of cell shown in C. **E:** Soma (E_1) and axon (E_2) of a beta cell for comparison with that of the topographically matched theta cell shown in D. Distance from soma to axonal segments illustrated is 0.4 mm in D_2 and 1.0 mm in E_2. **F, G:** High-power photomicrographs, differing only in focal plane, of a part of the dendritic arbor of the theta cell shown in B. Focus is on the outer arbor in F and on the inner arbor in G. The difference in focal plane is about 1.5 μm. **H, I:** A through-focus pair of micrographs as in F and G for the cell shown in A. Eccentricities (e) and distances from the visual streak (s) for illustrated cells as follows, with conventions as for Figure 1: A, H, and I: e = −3.5, s = −2.4; B, F, and G: e = +1.5, s = −1.3; C and D: e = +10.6, s = −7.6; E: e = +8.8, s = +4.1. Drawings of all three theta cells shown appear in Figure 1 (cell in A: Fig. 1I; cell in B: Fig. 1F; cell in C: Fig. 10). Scale bars = 100 μm in A–C; 25 μm in D–I; scale bar in E_2 applies to all four panels of D and E.

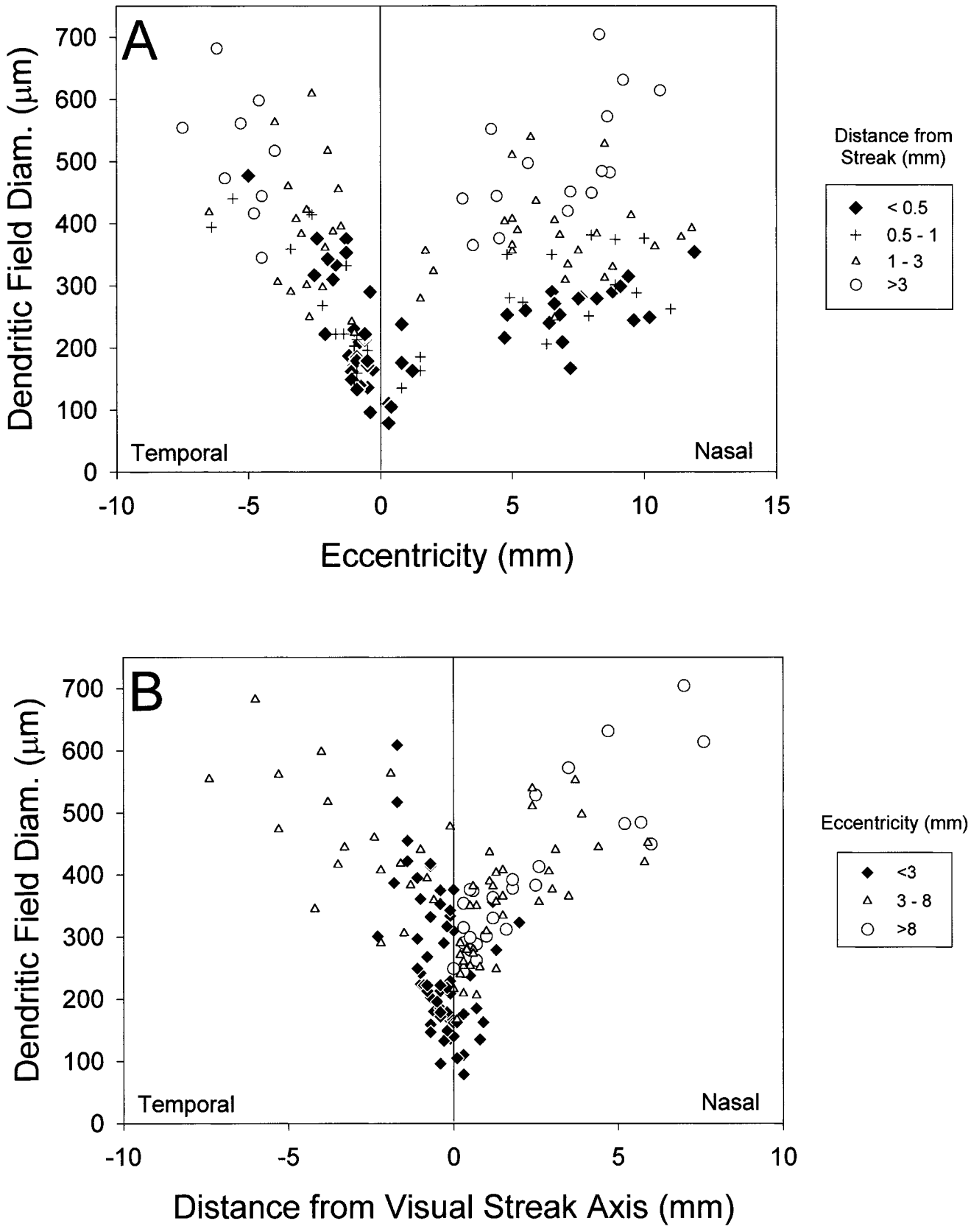
A
Dendritic Field Diam. (μm)
700
600
500
400
300
200
100
0
Temporal
Nasal
-10
-5
0
5
10
15
Eccentricity (mm)
Distance from Streak (mm)
< 0.5
0.5 - 1
1 - 3
>3
B
Dendritic Field Diam. (μm)
700
600
500
400
300
200
100
0
Temporal
Nasal
-10
-5
0
5
10
Distance from Visual Streak Axis (mm)
Eccentricity (mm)
<3
3 - 8
>8

Figure 4

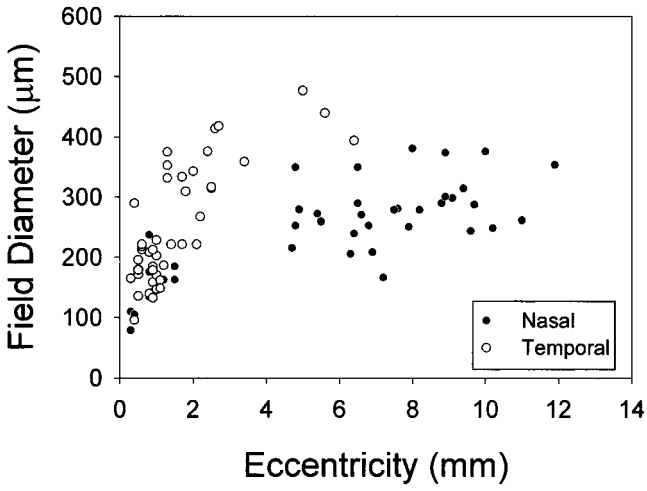

Fig. 5. Comparison of dendritic field sizes of theta cells in the nasal hemiretina (dots) with those in the temporal hemiretina (open circles). Only cells lying within 1 mm of the visual streak axis have been included. The absence of temporal cells at large eccentricities arises from the shorter horizontal extent of the temporal compared with the nasal hemiretina. Nasal cells are lacking at 2–4 mm eccentricity due to the difficulty of filling cells near the optic disk.

beta cells of the non-streak periphery (cf. Fig. 4A of this paper and Fig. 14 of Stein et al., 1996). Theta cells were smaller than virtually all epsilon cells (not shown; see Pu et al., 1994) and also smaller than delta cells on average, although with considerable overlap between the populations (Fig. 7B). Theta cells had slightly larger fields than zeta cells on average, but this distinction was far more evident in the temporal than in the nasal retina (Fig. 7B). Theta and eta cells were comparable in field size except in the peripheral nasal visual streak, where theta fields were smaller (not shown; cf. Fig. 4A of this paper and Fig. 4A of Berson et al., 1999). The proportional increase in field diameter from the area centralis to the nasal non-streak periphery (sixfold) was larger for theta cells than for alpha, delta, epsilon, zeta, and eta cells but somewhat smaller than for beta cells (more than eightfold; Boycott and Wässle, 1974; Kolb et al., 1981; Dacey, 1989; Pu et al., 1994; Berson et al., 1998).

Dendritic stratification

Theta cell dendritic arbors were narrowly bistratified, with an outer arbor in approximately stratum S2 of sublamina *a* and an inner arbor in S3/4 of sublamina *b*. This bistratification was not as obvious as for some other ganglion cell types (see, e.g., Amthor et al., 1984; Famiglietti, 1987; Dacey, 1993a) and on cursory inspection could be mistaken for a broadly unistratified arbor centered on the *a*/*b* sublaminar border. On closer observation, however, it was clear that most branches lay at one of two closely spaced levels within the IPL. These were interconnected at many points by branches coursing along more or less vertical trajectories.

Figure 8 illustrates this architecture for a theta cell of the central retina reconstructed by computer. In Figure 8A, the arbor is displayed as seen en face in the wholemounted retina, whereas in Figure 8B the arbor has been rotated 90° and displayed as if viewed along an axis in the plane of the retina. A large fraction of total dendritic length lies in two bands, one in the inner part of sublamina *a* and the other in the outer part of sublamina *b*. Many of the processes in these strata are horizontally disposed, whereas the dendrites that bridge the strata are predominantly oblique or near vertical. Figure 8B captures incompletely the narrowness of bistratification because the imperfect flatness of the tissue introduces noise in the depth measurements. For some cells this factor obscured almost completely the bistratified nature of the arbor. That it did not do so for the cell in Figure 8 is attributable to at least three factors: the retina was relatively flat in this region; the cell's dendritic field was small; and the separation between the inner and outer arbors was relatively wide because of the increased thickness of the IPL in the central retina.

To circumvent this limitation of the reconstruction method, we used an alternative method to examine the dendritic stratification. We determined the difference in depth between overlapping processes at each point of intersection in the dendritic profile as viewed en face in the wholemount. Such measurements sacrifice information about the absolute depth of the dendrites within the IPL, but because they are drawn from individual points on the retinal plane, they are unaffected by histological undulations in the wholemount. The histogram of Figure 8C displays the distribution of depth differences for the cell shown in Figure 8A and B. Note that the distribution is unimodal and sharply peaked at about 6 μm, with few instances of depth difference in the range 0–3 μm. This is as predicted for a bistratified arbor and not for a broadly unistratified arbor.

The histogram of Figure 9 shows the same sort of distribution of depth differences for a second theta cell, that illustrated in Figure 1H. Again, the distribution exhibits a major peak, in this case around 3–4 μm. The smaller average difference in depth between the inner and outer arbors in this case presumably reflects reduced IPL thickness at this more peripheral location. Individually, the inner and outer arbors (Fig. 9, bottom) exhibit much less dendritic overlap than does the entire profile (Fig. 9, top). A similar pattern typifies the ON-OFF direction selective (BS1) ganglion cell of rabbit retina (e.g., Amthor et al., 1984; Vaney et al., 1994). However, the theta cell does occasionally exhibit within-arbor overlap, and this accounts for the secondary peak at zero depth difference in the histogram. The notch between the peaks reflects the reduced density of dendritic branches in the gap between the inner and outer arbors.

To determine more accurately the level of stratification, we used through-focus methods to compare the depths of dendrites of theta cells with those of overlapping ON and OFF alpha cells. The outer tier of the bistratified theta cell arbor costratified almost completely with the dendrites of type *a* (OFF) alpha cells in S2, whereas the inner theta arbor costratified with dendrites of type *b* (ON) alpha cells in S3/4 (Figs. 10, 11). These observations were based on 20

Fig. 4. Dependence of theta-cell dendritic field size on retinal eccentricity and distance from the visual streak. **A:** Plot of field diameter as a function of eccentricity (i.e., radial distance from the area centralis). Each symbol type indicates a range of distance from the axis of the visual streak, as indicated in the key. **B:** Plot of field diameter as a function of distance from the visual streak axis. Each symbol type indicates a range of eccentricity, as indicated in the key. Negative values of eccentricity or streak distance denote locations in the temporal hemiretina. No distinction has been made between superior and inferior retina.

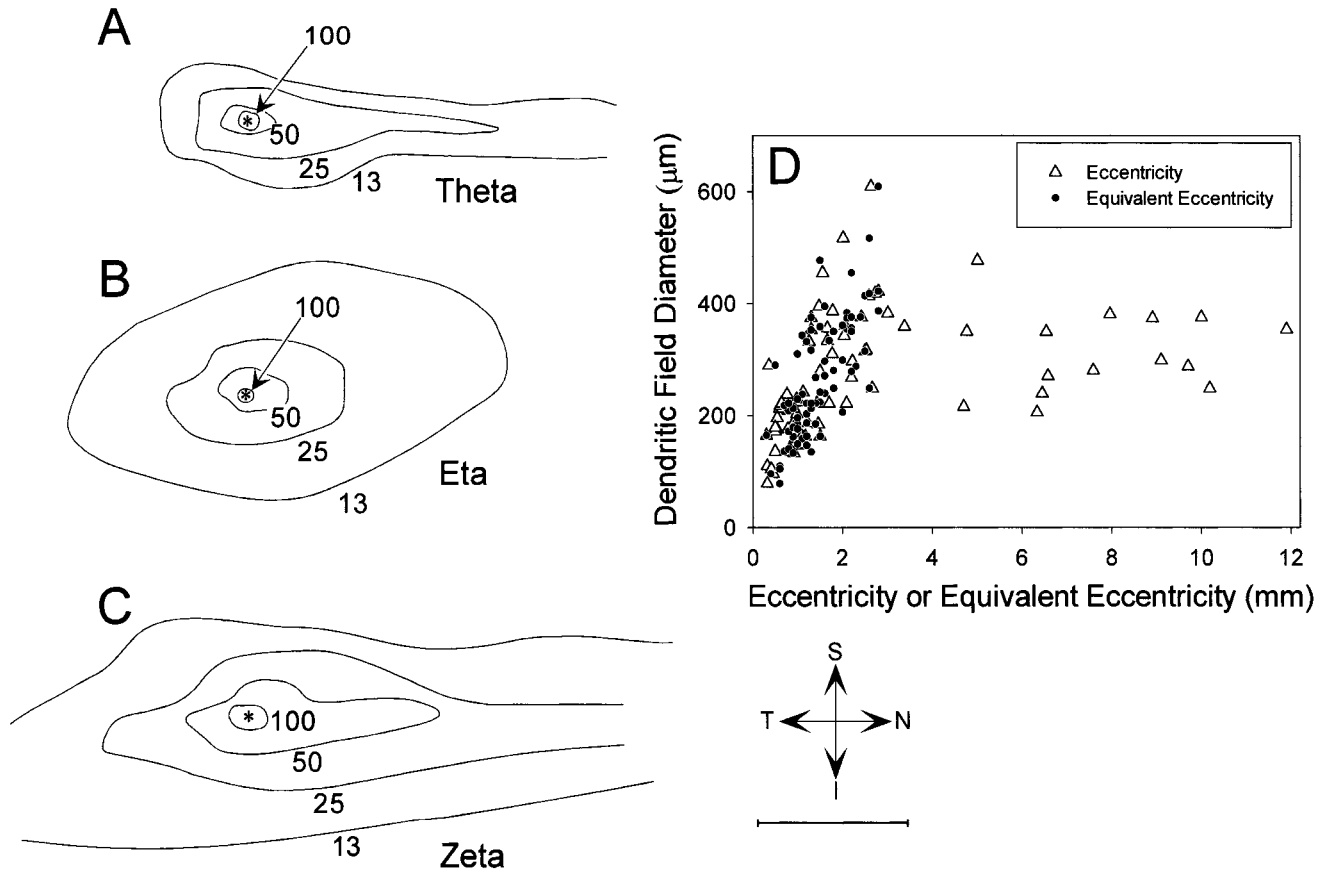

Fig. 6. **A–C:** Comparison of inferred retinal distributions of theta cells (A), eta cells (B), and zeta cells (C) of the cat retina. Density estimates obtained for all three cell types by assuming a constant dendritic coverage (field area × local density) of 1. Data for theta cells based on a sample of 261 dendritic fields. Plots are aligned vertically at the areae centrales (asterisks), where peak densities reach 202 cells/mm^2 for theta cells, 146 cells/mm^2 for eta cells, and 378 cells/mm^2 for zeta cells. S, superior; I, inferior; N, nasal; T, temporal. **D:** Evidence that the plot in A accounts for most of the topographic variation in dendritic field size among theta cells. The plot employs a transform of eccentricity, termed equivalent eccentricity, which compensates for radial asymmetries in the density distribution (see text and Watanabe and Rodieck, 1989 for details). The standard path used to define equivalent eccentricity ran from the area centralis to the temporal periphery and was coaxial with the nasal visual streak. Each cell lying within the 13 cells/mm^2 isodensity contour is plotted twice, once at its eccentricity (open triangle) and again at its equivalent eccentricity (dot). To obtain local density estimates, we derived from A spline-fit plots of density against distance for the standard path and for other polar angles sampled at 5–10° intervals. Density values for sites lying between these polar traverses were obtained from the plots by linear interpolation. Temporal as well as nasal sites have been assigned positive values of eccentricity. (Data for B and C reproduced with permission from Berson et al., 1998, 1999.) Scale bar = 5 mm in A–C.

theta cells, of which 7 overlapped both ON and OFF alpha cells and 13 overlapped one of the two types.

Depth comparisons with other ganglion cell types confirmed the foregoing analysis. Delta (monoamine-accumulating) cells are known to ramify exclusively in S1 (Dacey, 1989 and our unpublished observations; but see Wässle et al., 1987). In the one instance of overlap observed, the theta cell's outer arbor ramified just beneath (i.e., vitread to) the dendrites of an overlapping delta cell. The dendrites of zeta cells stratify narrowly near the *a*/*b* sublaminar border (Berson et al., 1998). In two instances of overlap, theta cell arbor was centered at about the same depth as that of the zeta cell, but ramified both above and below it. OFF beta cells stratify broadly in sublamina *a* and ON beta cells mainly in S3 and S4 (Famiglietti and Kolb, 1976; Watanabe et al., 1985; McGuire et al., 1986; Weber et al., 1991). The outer tier of theta cell dendrites costratified with the lower part of OFF beta arbors (n = 3), whereas the inner tier of the theta cell arbor ramified with the upper part of the ON beta arbor (n = 1). Epsilon cells (n = 9), which are known to occupy S3 and S4 (Pu et al., 1994), stratified with and somewhat below the inner arbor of theta cells. Together, these data support other evidence that theta cell dendrites arborize primarily in two strata, corresponding to about S2 and S3/4, linked by branches traversing the gap between them.

Central projections

Theta cells were commonly encountered among cells labeled by retrograde transport from the superior colliculus (n = 41; see Fig. 1G and L for examples) and from the

Fig. 7. Comparison of dendritic field sizes of theta cells (filled diamonds in both panels) with those of other types of cat ganglion cells. **A:** Comparison of theta cells with alpha cells (open circles) and beta cells (dots). **B:** Comparison of theta cells with delta (monoamine-accumulating) cells (open triangles) and zeta cells (open squares). Other conventions as for Figure 4.

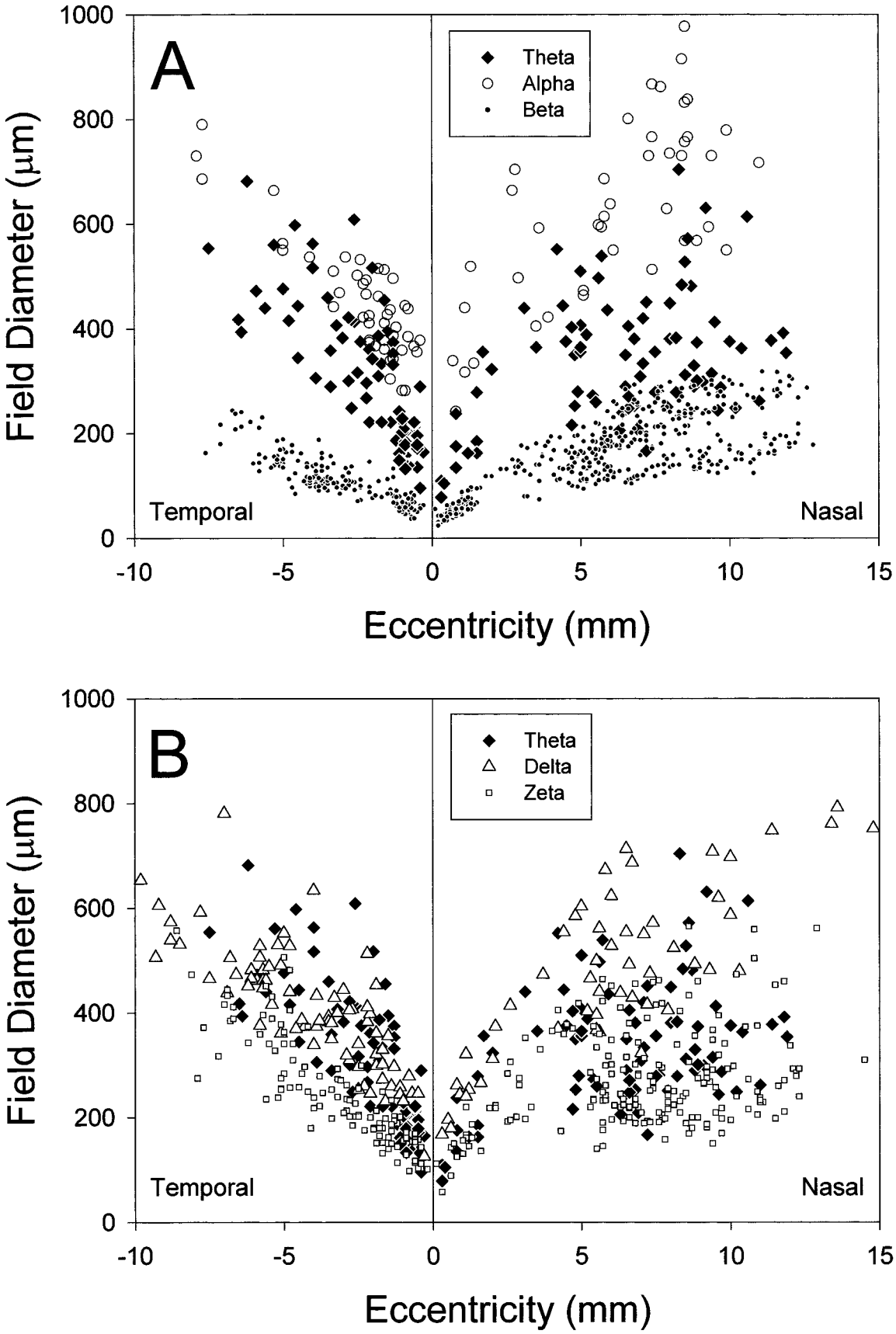
A
Theta
Alpha
Beta
Temporal
Nasal
Field Diameter (µm)
Eccentricity (mm)
1000
800
600
400
200
0
-10
-5
0
5
10
15
B
Theta
Delta
Zeta
Temporal
Nasal
Field Diameter (µm)
Eccentricity (mm)

Figure 7

medial interlaminar nucleus (n = 16; e.g., Fig. 1J) and C-laminae (n = 8) of the lateral geniculate nucleus. Theta cells were never encountered among >300 cells labeled from the A-layers of the lateral geniculate nucleus nor among >150 labeled from the geniculate wing. Theta cells appeared to have uncrossed projections from the temporal retina. Twenty-nine theta cells were among the several hundred temporal retinal cells labeled from the ipsilateral superior colliculus or geniculate complex whereas none were among a much smaller sample of temporal cells labeled from the contralateral colliculus.

DISCUSSION

We have defined a new morphological type of ganglion cell of the cat retina, the theta cell. Its salient morphological features include a densely branched, bistratified dendritic arbor, a small soma, and a slender axon. Theta cells innervate both the midbrain tectum and visual thalamus and project ipsilaterally from the temporal retina.

Relationship to other cat ganglion cell types

The theta cell is clearly distinct from the eight other well-studied morphological ganglion cell types of the cat retina: the ON and OFF alpha cells; the ON and OFF beta cells; and the delta (monoamine-accumulating), epsilon, zeta, and eta cells (Fig. 12). Each of these appears to represent a "natural type" (Rodieck and Brening, 1983) whose members covary on a large number of dimensions, including soma size, axon caliber, field size, frequency of dendritic branching and overlap, dendritic stratification, and patterns of central projection. The distinctions between theta cells and other cell types are apparent to some extent in the one- or two-dimensional plots of Figures 3B and 7A and B (see also Figs. 10, 11, and 12), although types are best recognized by simultaneous consideration of many more dimensions (Rodieck and Brening, 1983).

As a practical matter, most established ganglion cell types can be differentiated from theta cells by considering a small set of features (Fig. 12). Alpha cells are readily distinguishable from theta cells on the basis of soma size (Fig. 3B) or axonal caliber alone and from the relationship between dendritic field size and eccentricity (Fig. 7A). Unlike theta cells, they are narrowly unistratified and have radiate dendritic profiles with little overlap. Beta cells are easily distinguished from theta cells on the basis of dendritic field size if topographic location is also known (Fig. 7A). In addition, beta cell dendritic trees differ from those of theta cells in being unistratified, with broad arborizations either in sublamina *a* (OFF betas) or in sublamina *b* (ON betas). In the absence of reliable data on stratification or topography, beta cells can be distinguished reasonably well from theta cells on the basis of their relatively small dendritic fields (<200 μm diameter), larger somata, or relatively thick axons. Epsilon and delta cells differ markedly from theta cells in their much lower branching density and in their unistratified patterns of dendritic arborization (Fig. 12). Epsilon cells also have larger dendritic fields than theta cells at any eccentricity (cf. Fig. 7 and Pu et al., 1994).

Zeta and eta cells are more difficult to distinguish from theta cells because of their substantial mutual overlap on several of the dimensions considered in this report (Berson et al., 1998, 1999). All three types have tufted dendritic profiles with relatively high branching density and dendritic field diameters of intermediate size among cat ganglion cells. All three have similar soma sizes and axon calibers. Definitive discrimination of these three types thus depends primarily on close inspection of dendritic structure and particularly of dendritic stratification patterns.

Zeta cells (Berson et al., 1998) have narrowly unistratified arbors ramifying near the *a*/*b* sublaminar border. In the periphery of the arbor, dendrites rarely overlap one

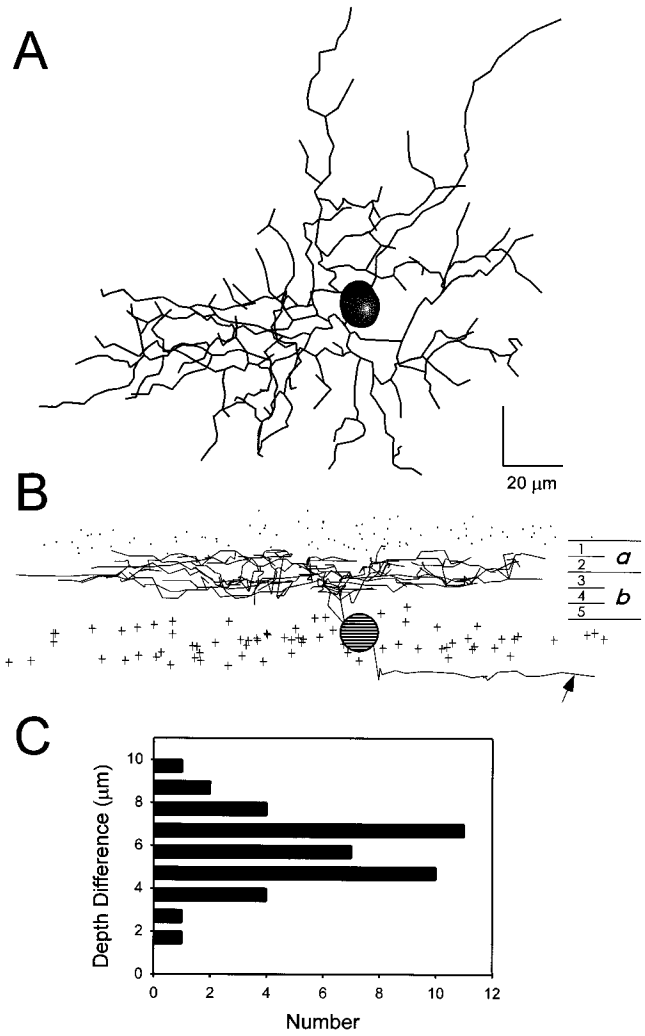

Fig. 8. Dendritic stratification of a theta cell of the central retina as revealed by computer reconstruction. This cell was selected for reconstruction because the relatively small size of its dendritic field reduced the distorting effect of imperfect retinal flatness on the uniformity of depth information in such views. Cell lay 0.4 mm superior to the area centralis. **A:** Reconstructed profile displayed en face, as if viewed in the wholemount. Axon omitted for clarity. **B:** Same profile after 90° rotation about an axis lying in the plane of the retina to generate a vertical view. Cell body appears as a hatched circle, and dendrites appear as straight line segments. Arrow indicates axon. Plusses indicate depth of other somata of the ganglion cell layer, and dots mark the position of dark granules found at the outer margin of the inner plexiform layer (see Materials and Methods). Numbers at right indicate approximate depth of strata of the inner plexiform layer, and *a* and *b* denote the OFF and ON sublayers, respectively. **C:** Distribution of differences in depth between pairs of overlapping dendritic processes, measured at their point of intersection when viewed en face, as in A. Except for bifurcations of single processes, every such intersection was included in the analysis. Scale bar = 20 μm in vertical as well as horizontal dimensions of B and also applies to A.

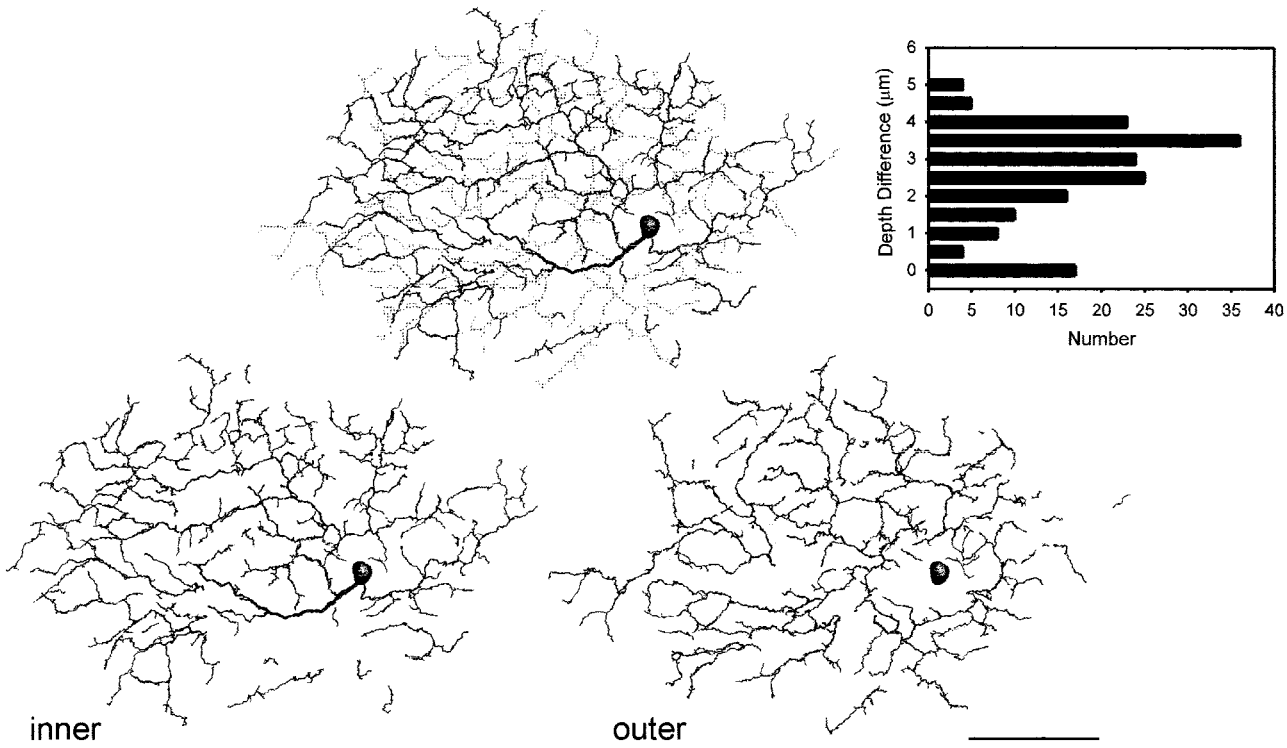

Fig. 9. Analysis of the structure and separation in depth between the inner and outer dendritic arbors of the theta cell illustrated in Figure 1H. Separate camera lucida drawings are shown below of the dendritic segments located in each of the two levels of stratification. The two profiles have been superimposed above, with solid branches representing the inner arbor and stippled ones the outer arbor. Histogram plots the differences in depth between dendrites at all points of overlap in this profile, as in Figure 8C. The secondary peak at zero depth difference reflects occasional overlap among dendrites within the same tier. This cell lay 1.8 mm superior to the area centralis.

another and when they do are almost never separated in depth by more than a micrometer. By contrast, theta cell dendrites overlap one another at many points throughout the field and are separated in depth by a characteristic distance (2–6 μm, depending on eccentricity). The great majority of theta cell dendrites lie in two strata corresponding closely to the levels occupied by the dendrites of ON and OFF alpha cells. By contrast, nearly all zeta cell dendrites ramify in between these two alpha cell strata. Zeta cells also apparently project contralaterally from the temporal retina and have little if any thalamic projection, whereas theta cells project ipsilaterally from the temporal retina and innervate several components of the lateral geniculate complex.

Of well-established types, eta cells (Berson et al., 1999) are the most likely to be mistaken for theta cells. These two types have similar field dimensions, soma sizes, and axon calibers, as noted above. Both typically exhibit extensive dendritic overlap when viewed en face, and their arbors span about the same vertical extent of the IPL. However, eta cells lack the bistratification of theta cells, so that there is no characteristic separation in depth between overlapping dendrites (Fig. 11G). Moreover, eta cell arbors are displaced upward in the IPL relative to those of theta cells. In particular, eta cell dendrites encroach on the upper part of sublamina *a* (S1), which theta arbors do not, and largely avoid sublamina *b*, where the inner stratum of theta dendrites arborize extensively. As a rule, eta cell profiles are relatively radiate and orderly whereas theta profiles are more tangled and chaotic, with a higher density of short terminal branches.

Besides the well-established types described above, a great variety of less thoroughly studied morphological forms has been depicted in earlier reports on cat ganglion cells (e.g., Boycott and Wässle, 1974; Stone and Clarke, 1980; Kolb et al., 1981; Saito, 1983; Fukuda et al., 1984; Famiglietti, 1987; Stanford, 1987; Ramoa et al., 1988; Tootle, 1993). None of these appears to correspond to the theta cell. Perhaps the closest match is a bistratified type presumed to correspond to the ON-OFF direction-selective cell (Famiglietti, 1987) and also known as the iota cell (Berson et al., 1997). Theta and iota cells arborize at virtually identical levels of the IPL. However, iota cells have by comparison with theta cells sparser dendritic branching, fewer links between inner and outer arbors, and slightly larger fields in the nasal retina (Berson et al., 1997). Emerging evidence also suggests that theta and iota cells differ functionally in their sensitivity to stimulus direction (see below). A bistratified variety termed G11 by Kolb et al. (1981) has a substantially smaller dendritic field than the theta cell and arborizes at different levels of the IPL.

Likely homologues of the theta cell in other mammalian retinas

A ganglion cell virtually indistinguishable from the theta cell is present in the retina of the ferret, another member of the order Carnivora. It has a small soma, a fine axon, and a highly branched, narrowly bistratified dendritic field that costratifies with the ON and OFF alpha cells (Isayama et al., 1998). Ferret theta cells appear to have been included among the "tight" ganglion cells of

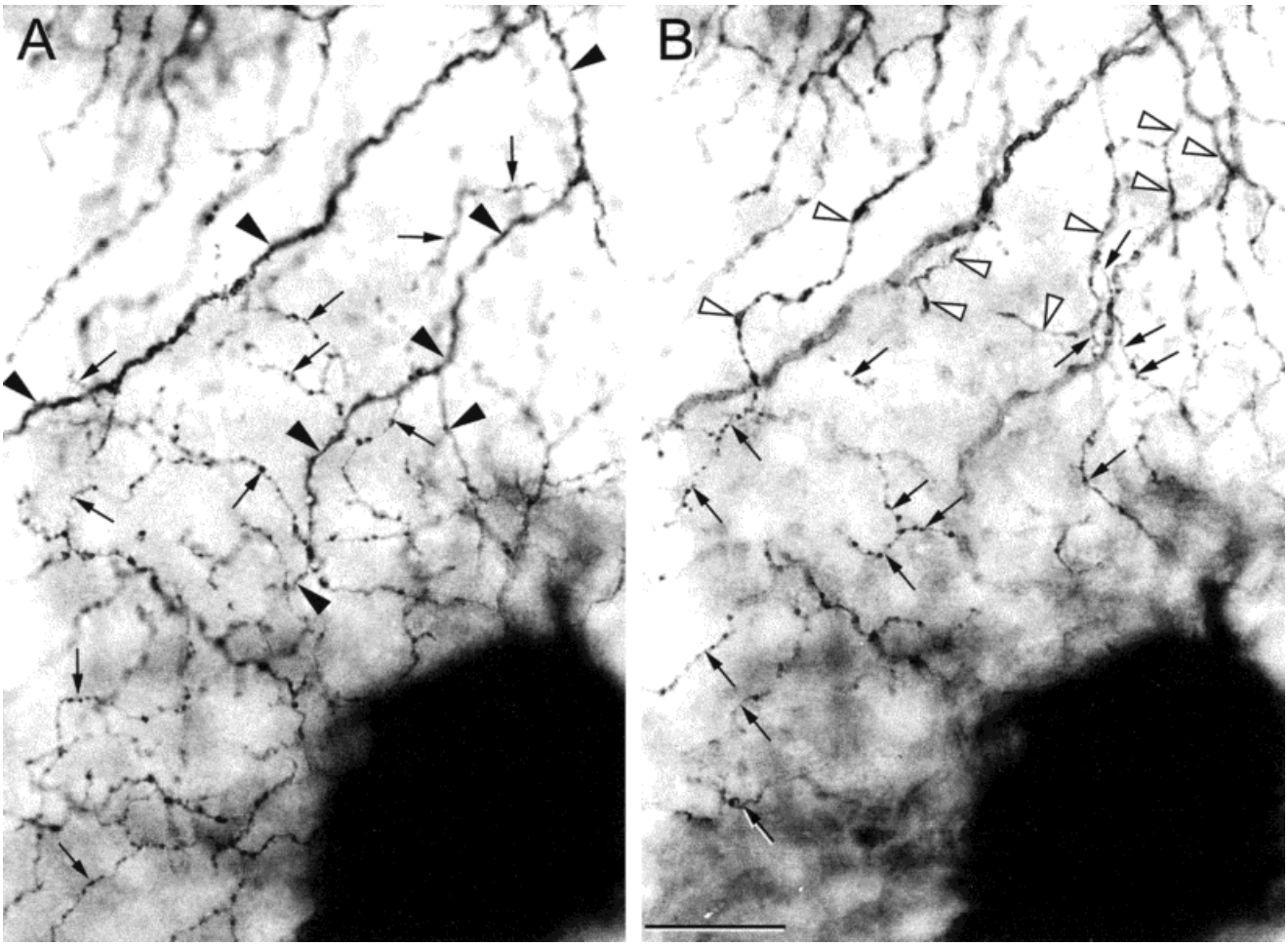

Fig. 10. **A, B:** Pair of photomicrographs at different focal planes comparing depth of dendritic stratification of a theta cell, an ON-alpha cell, and an OFF-alpha cell with mutually overlapping arbors. Plane of focus in A is above (sclerad) to that in B and corresponds to the level of stratification of the OFF alpha cell's dendrites (filled arrowheads) and of the outer tier of theta cell dendrites (arrows). Focal plane in B lies approximately 3 μm below (vitread to) that in A and corresponds to the level of stratification of the ON alpha dendrites (open arrowheads) and also of the inner tier of dendrites of the theta cell (arrows). In this part of the dendritic field the outer arbor of the theta cell was more densely branching than the inner arbor. Further data on this set of overlapping cells appear in Figure 11. The theta cell lay 1.4 mm from the area centralis and 0.9 mm from the visual streak axis in the inferior temporal retina. Scale bar = 25 μm in B.

Wingate et al. (1992), a heterogeneous group of cells that also seems to have included ferret counterparts of the zeta and eta types (for details, see Isayama et al., 1998; Berson et al., 1998, 1999). Theta cells in cat contribute to the ipsilateral retinal projection to the midbrain and thalamus, but "tight" cells in the ferret reportedly do not (Win-

Fig. 11. **A–F:** Comparisons of depth of dendritic stratification of the three cells with overlapping arbors shown in Figure 10: a theta cell, an ON alpha cell, and an OFF alpha cell. **A:** Camera lucida drawings of the three cells. Central box shows the full somadendritic profile of the OFF alpha cell and the somata of the other two cells in their actual spatial relationship. The drawings of the dendritic profiles of the other two cells have been shifted laterally (arrows) so that their morphology can be viewed in isolation. Axons omitted for clarity. **B–F:** Quantitative analysis of relative depth of stratification of these cells. B: Depth of dendrites of the theta cell (open diamonds) and ON-alpha cell (open circles) referenced to the depth of overlapping OFF-alpha cell dendrites (dotted line). Each point represents the depth of a dendrite at an intersection between the dendritic profiles of two of these cells. Data are plotted as a function of linear distance on the retina to produce a view comparable to that in radial sections or in Figure 8B. The dendrites of the theta cell can be seen to costratify with those of both the ON and OFF alpha cells. Vertical dimension has been expanded, as reflected in scale bar. C: Depth of dendrites of the theta cell (open diamonds) and OFF-alpha cell (filled circles) referenced to the depth of overlapping ON-alpha cell dendrites (dotted line). Scale same as in B. D, E: Histogram displays of the normalized depth data for the theta cell from B and C, respectively. F: Histogram plotting (as for Figs. 8C and 9) differences in depth between dendrites of the theta cell (black bars) at points of intersection in the profile viewed en face. Hatched bars show, for comparison, the depth differences between dendrites of the ON- and OFF-alpha cells where their profiles intersect.). **G:** Histogram of differences in depth between overlapping dendrites of a single ganglion cell of the eta type, as for Figure 8C. Note that this histogram, unlike those for theta cells (Figs. 8C, 9, 11F), provides no evidence for dendritic bistratification. This eta cell had a dendritic field diameter of 480 μm and lay 8.5 mm from the area centralis and 6.5 mm from the visual streak in the superior nasal retina. Scale bar = 100 μm in A.

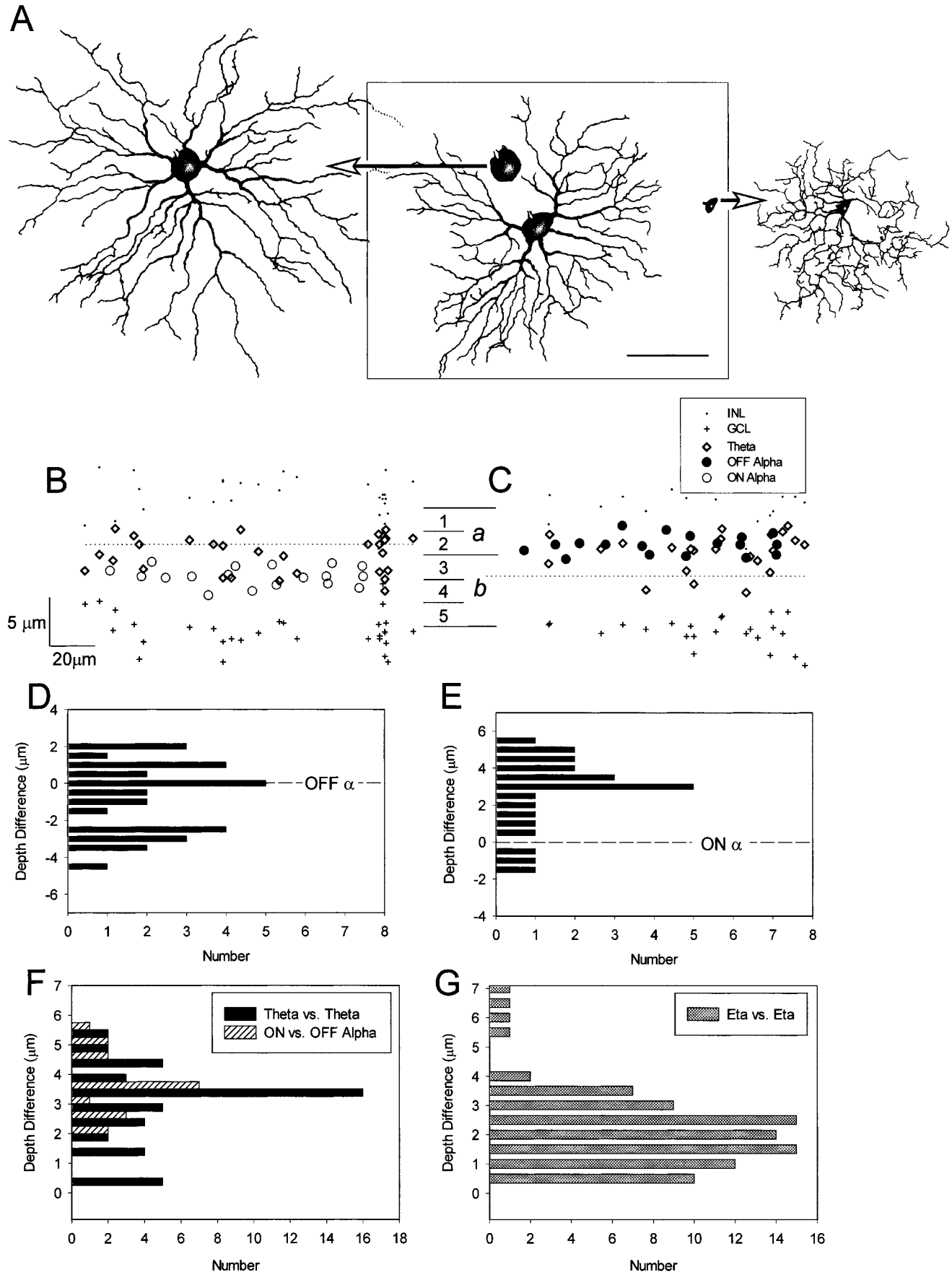
A
B
C
INL
GCL
Theta
OFF Alpha
ON Alpha
1
2
a
3
4
b
5
5 µm
20µm
D
Depth Difference (µm)
OFF α
Number
E
Depth Difference (µm)
ON α
Number
F
Theta vs. Theta
ON vs. OFF Alpha
Depth Difference (µm)
Number
G
Eta vs. Eta
Depth Difference (µm)
Number

Figure 11

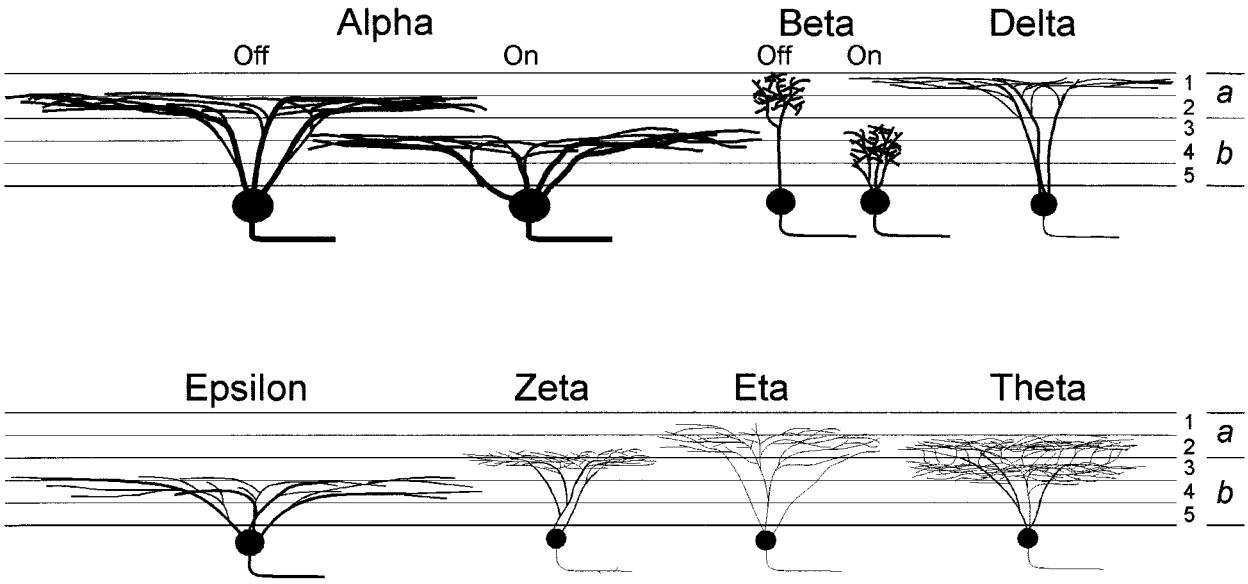

Fig. 12. Schematic summary comparing depth of dendritic stratification and relative dendritic field size of major morphological types of ganglion cells in cat retina. Laminar designations for the inner plexiform layer as for Figure 8.

gate et al., 1992). However, it is unclear whether this reflects a real difference between cat and ferret theta cells because the sample of ferret "tight" cells was small and apparently included types other than theta.

The theta cell may well have a homolog in primate retina. Many of the "T-group" ganglion cells described by Rodieck and Watanabe (1993) had fully bistratified dendritic arbors in sublayers *a* and *b*, densely branching and highly overlapping dendritic profiles, and projections to the superior colliculus (see especially the three most densely branching cells of their Fig. 8). A similar cell has been encountered in human retina by Peterson and Dacey (1999). Surveys of ganglion cell morphology in the rabbit retina (Famiglietti, 1992a,b; Amthor et al., 1989a,b) include no obvious equivalents of the theta cell.

Distribution, incidence, and total numbers of theta cells

Although we have no direct evidence on the retinal distribution of theta cells, the form of their density distribution may be inferred from the topography of their dendritic field sizes (Fig. 6) by assuming that their dendritic field overlap or coverage factor (field area × local density) is constant across the retina and at least 1 (Peichl and Wässle, 1979; Wässle et al., 1981; Dann et al., 1988; Dacey, 1989, 1993b; Vaney, 1994; Stein et al., 1996). If the actual value of theta coverage is greater than 1, as it appears to be for most cat ganglion cell types (Peichl and Wässle, 1979; Wässle et al., 1981; Dacey, 1989; Stein et al., 1996; Berson et al., 1998), the plot of Figure 6A would proportionally underestimate densities but would not distort the form of the distribution. That distribution shows a striking concentration of theta cells in the visual streak, the elongated region of relatively high ganglion cell density near the horizontal meridian of the nasal hemiretina (e.g., Wong and Hughes, 1987). The salience of the streak varies substantially among cat ganglion cell types. It is weakly expressed among delta, eta, and alpha cells (Fig. 11, bottom left; Wässle et al., 1975; Hughes, 1981; Dacey, 1989; Berson et al., 1999), more strongly developed for beta cells (Stein et al., 1996), and still more prominent among zeta cells (Fig. 6C; Berson et al., 1998). Along this spectrum, theta cells appear comparable to zeta cells in their pronounced tendency to concentrate in the streak.

Theta cells also appear comparable to zeta cells in having a moderately well-developed central retinal specialization. From the middle of the area centralis to the far peripheral nasal streak, theta cell field area increases about 14-fold (figured from the increase in mean diameter from about 80 to 300 μm). Zeta cells exhibit a similar increase of about 16-fold (Berson et al., 1998). These increases are larger than seen among eta cells (~4–5-fold; Berson et al., 1999) or delta cells (~11-fold; Dacey, 1989), but smaller than observed for beta cells (~36-fold; Stein et al., 1996).

Theta cells appear to have a greater nasotemporal asymmetry in density than any known ganglion cell type. Their dendritic field areas are fully 250% larger in the temporal hemiretina than in the nasal hemiretina (compared at 5-mm eccentricity on the visual streak axis). The difference is only 90% for zeta cells, 30% for eta cells, and 6% for beta cells (Stein et al., 1996; Berson et al., 1998, 1999). The value for delta cells is about 50% (Dacey, 1989) and for alpha cells between 0% and 35% (Wässle et al., 1975; Hughes, 1981), assuming density is inversely proportional to field area.

Integration of the inferred theta cell density distribution (Fig. 6A) yields an estimated total of 4300 theta cells per retina. This amounts to 3% of the estimated total ganglion cell population of about 160,000 (Williams et al., 1983; Chalupa et al., 1984). This should be viewed as a lower bound estimate since it is based on a conservative estimate of theta cell coverage.

Physiological identity

Intracellular recordings in vitro from several identified cat theta cells indicate that they are excited transiently by both

increments and decrements in center illumination and that they are insensitive to stimulus direction (O'Brien et al., 1999). These features are characteristic of a particular variety of "sluggish" ganglion cell or "W-cell" variously designated as the ON-OFF phasic W cell (Stone and Fukuda, 1974), the local edge detector (Cleland and Levick, 1974b), or the "impressed by contrast" cell (Troy et al., 1989).

The anatomy of theta cells largely supports this proposed correspondence. They have among the smallest somata and thinnest axons of all cat ganglion cells (Dacey, 1989; Pu et al., 1994; and unpublished observations) and thus presumably have among the slowest conduction velocities. They project to the superior colliculus and to the medial interlaminar nucleus and C-layers of the lateral geniculate nucleus, but not to the A-layers. They ramify in both the *a* and *b* sublaminae of the IPL and are thus in a position to receive excitatory input from both ON and OFF bipolar cells. Of the established physiological types of cat ganglion cells, only two share all these features: the ON-OFF phasic cells and the ON-OFF direction-selective cells (Cleland and Levick, 1974a,b; Rowe and Stone, 1977; Stone, 1983; Stanford, 1987; Troy et al., 1989; Rowe and Palmer, 1995). The direction-selective cell appears to correspond to a distinct morphological type termed the iota cell (Famiglietti, 1987; Berson et al., 1997; O'Brien, Isayama and Berson, unpublished observations). Thus, on anatomical grounds alone, the theta cell seems most likely to correspond to an ON-OFF phasic cell, in agreement with the preliminary physiological evidence (O'Brien et al., 1999).

If confirmed, this would imply that ON-OFF phasic W-cells (or local edge detectors) are associated with at least two distinct morphological types of ganglion cells: the theta cell and the zeta cell (Berson et al., 1998; O'Brien et al., 1999). It will be of interest to learn whether these types can be distinguished functionally and, if so, what accounts for the distinctions. In structural terms, the two types are similar in many respects: both have small somas and thin axons, relatively small dendritic fields, and a strong tendency to concentrate in the nasal visual streak. Differences in dendritic stratification, however, suggest that the two types may be affiliated with at least partly distinct sets of amacrine and bipolar cells.

Clues to functional specialization may also lie in the different outputs of the two types. Although both project to the superior colliculus, theta cells differ from zeta cells in making a substantial contribution to the ipsilateral retinofugal pathway and to the retinogeniculate projection. The theta cell's ipsilateral temporal projection seems at odds with evidence from antidromic studies that the great majority of ON-OFF phasic cells have crossed projections from the temporal as well as the nasal retina (Kirk et al., 1976). The basis for the discrepancy is unclear, but it may reflect a bias against recording from theta cells in extracellular studies. The thalamic projection of theta cells may be partly responsible for the presence of ON-OFF center phasic cells in the C-laminae of the lateral geniculate (Sur and Sherman, 1982), since these are likely to be driven by input from ganglion cells with similar receptive field structure.

ACKNOWLEDGMENTS

We thank Shane Johnson for his assistance on some of the retrograde tracing experiments; Mike Paradiso and Cindi Rittenhouse for donations of cat eyes; and Brendan O'Brien and David Wells for assistance with digital imaging.

LITERATURE CITED

Amthor FR, Oyster CW, Takahashi ES. 1984. Morphology of on-off direction-selective ganglion cells in the rabbit retina. Brain Res 298:187–190.

Amthor FR, Takahashi ES, Oyster CW. 1989a. Morphologies of rabbit retinal ganglion cells with complex receptive fields. J Comp Neurol 280:97–121.

Amthor FR, Takahashi ES, Oyster CW. 1989b. Morphologies of rabbit retinal ganglion cells with concentric receptive fields. J Comp Neurol 280:72–96.

Berson DM, Isayama T, Pu M. 1997. Morphology of presumed ON-OFF direction selective ganglion cell of cat retina. Soc Neurosci Abstr 23:730.

Berson DM, Pu M, Famiglietti EV. 1998. The zeta cell: a new ganglion cell type of the cat retina. J Comp Neurol 399:269–288.

Berson DM, Isayama T, Pu M. 1999. The eta ganglion cell type of cat retina. J Comp Neurol 408:204–219.

Boycott BB, Wässle H. 1974. The morphological types of ganglion cells of the domestic cat's retina. J Physiol (Lond) 240:397–419.

Chalupa LM, Williams RW, Henderson Z. 1984. Binocular interaction in the fetal cat regulates the size of the ganglion cell population. Neurosci 12:1139–1146.

Cleland BG, Levick WR. 1974a. Brisk and sluggish concentrically organized ganglion cells in the cat's retina. J Physiol (Lond) 240:421–456.

Cleland BG, Levick WR. 1974b. Properties of rarely encountered types of ganglion cells in the cat's retina and an overall classification. J Physiol (Lond) 240:457–492.

Dacey DM. 1989. Monoamine-accumulating ganglion cell type of the cat's retina. J Comp Neurol 288:59–80.

Dacey DM. 1993a. Morphology of a small-field bistratified ganglion cell type in the macaque and human retina. Vis Neurosci 10:1081–1098.

Dacey DM. 1993b. The mosaic of midget ganglion cells in the human retina. J Neurosci 13:5334–5355.

Dann JF, Buhl EH, Peichl L. 1988. Postnatal dendritic maturation of alpha and beta ganglion cells in cat retina. J Neurosci 8:1485–1499.

Famiglietti EV. 1987. Starburst amacrine cells in cat retina are associated with bistratified, presumed directionally selective, ganglion cells. Brain Res 413:404–408.

Famiglietti EV. 1992a. Dendritic co-stratification of ON and ON-OFF directionally selective ganglion cells with starburst amacrine cells in rabbit retina. J Comp Neurol 324:322–335.

Famiglietti EV. 1992b. New metrics for analysis of dendritic branching patterns demonstrating similarities and differences in ON and ON-OFF directionally selective retinal ganglion cells. J Comp Neurol 324: 295–321.

Famiglietti EV, Kolb H. 1976. Structural basis for 'ON' and 'OFF'-center responses in retinal ganglion cells. Science 194:193–195.

Fukuda Y, Hsiao C-F, Watanabe M, Ito H. 1984. Morphological correlates of physiologically identified Y-, X-, and W-cells in the cat retina. J Neurophysiol 52:999–1013.

Hughes A. 1977. Topography of vision in mammals of contrasting life style: comparative optics and retinal organisation. In: Crescitelli F, editor. Visual system in evolution in vertebrates. Handbook of sensory physiology, vol 7, no 5. Berlin: Springer-Verlag. p 613–756.

Hughes A. 1981. Population magnitudes and distribution of the major modal classes of retinal ganglion cell as estimated from HRP filling and a systematic survey of the soma diameter spectra for classical neurones. J Comp Neurol 197:303–339.

Isayama T, O'Brien B, Ugalde I, Frenz A, Aurora V, Tsiaras W, Muller J, Berson D. 1998. Morphology of ferret retinal ganglion cells. Invest Ophthalmol Visual Sci (Suppl) 39:S563.

Kirk DL, Levick WR, Cleland BG. 1976. The crossed or uncrossed destination of axons of sluggish concentric and non-concentric cat retinal ganglion cells, with an overall synthesis of the visual field representation. Vision Res 16:233–236.

Kolb H, Nelson R, Mariani, A. 1981. Amacrine cells, bipolar cells and ganglion cells of the cat retina: a Golgi study. Vision Res 21:1081–1114.

Leventhal AG, Keens J, Törk I. 1980. The afferent ganglion cells and cortical projections of the retinal recipient zone (RRZ) of the cat's 'pulvinar complex.' J Comp Neurol 194:535–554.

McGuire BA, Stevens JK, Sterling P. 1986. Microcircuitry of beta ganglion cells in cat retina. J Neurosci 6:907–918.

O'Brien BJ, Isayama T, Berson DM. 1999. Light responses of morphologically identified cat ganglion cells. Invest Ophthalmol Vis Sci 40:S815

Peichl L, Wässle H. 1979. Size, scatter, and coverage of ganglion cell receptive field centers in the cat retina. J Physiol (Lond) 291:117–141.

Peterson BB, Dacey DM. 1999. Morphology of wide-field bistratified and diffusely stratified human retinal ganglion cells. Invest Ophthalmol Vis Sci 40:S814.

Pu M, Berson DM. 1991. Morphology of ganglion cells innervating the medial interlaminar nucleus of the lateral geniculate body. Soc Neurosci Abstr 17:709.

Pu M, Berson DM. 1992. A method for reliable and permanent intracellular staining of retinal ganglion cells. J Neurosci Methods 41:45–51.

Pu M, Berson DM, Pan T. 1994. Structure and function of retinal ganglion cells innervating the cat's geniculate wing: an *in vitro* study. J Neurosci 14:4338–4358.

Ramoa AS, Campbell G, Shatz CJ. 1988. Dendritic growth and remodeling of cat retinal ganglion cells during fetal and postnatal development. J Neurosci 8:4239–4261.

Ramón-Moliner E. 1962. An attempt at classifying nerve cells on the basis of their dendritic patterns. J Comp Neurol 119:211–227.

Rodieck RW. 1998. The first steps in seeing. Sunderland, MA: Sinauer Associates.

Rodieck RW, Brening RK. 1983. Retinal ganglion cells: properties, types, genera, pathways and trans-species comparisons. Brain Behav Evol 23:121–164.

Rodieck RW, Watanabe M. 1993. Survey of the morphology of macaque retinal ganglion cells that project to the pretectum, superior colliculus, and parvicellular laminae of the lateral geniculate nucleus. J Comp Neurol 338:289–303.

Rowe MH, Palmer LA. 1995. Spatio-temporal receptive-field structure of phasic W cells in the cat retina. Vis Neurosci 12:117–139.

Rowe MH, Stone J. 1977. Naming of neurons: classification and naming of cat retinal ganglion cells. Brain Behav Evol 14:185–216.

Saito AH. 1983. Morphology of physiologically identified X-, Y-, and W-type retinal ganglion cells of the cat. J Comp Neurol 221:279–288.

Stanford LR. 1987. W-cells in the cat retina: correlated morphological and physiological evidence for two distinct classes. J Neurophysiol 57:218–244.

Stein JJ, Johnson SA, Berson DM. 1996. Distribution and coverage of beta cells in the cat retina. J Comp Neurol 372:597–617.

Stone J. 1983. Parallel processing in the visual system: the classification of retinal ganglion cells and its impact on the neurobiology of vision. New York: Plenum.

Stone J, Clarke RM. 1980. Correlation between soma size and dendritic morphology in cat retinal ganglion cells: evidence of further variation in the gamma-cell class. J Comp Neurol 192:211–218.

Stone J, Fukuda Y. 1974. Properties of cat retinal ganglion cells: a comparison of W-cells with X- and Y-cells. J Neurophysiol 37:722–748.

Sur M, Sherman SM. 1982. Linear and non-linear W-cells in C-laminae of the cat's lateral geniculate nucleus. J Neurophysiol 47:869–884.

Tootle JS. 1993. Early postnatal development of visual function in ganglion cells of the cat retina. J Neurophysiol 69:1645–1660.

Troy JB, Einstein G, Schuurmans RP, Robson JG, Enroth-Cugell C. 1989. Responses to sinusoidal gratings of two types of very nonlinear retinal ganglion cells of cat. Vis Neurosci 3:213–223.

Vaney DI. 1994. Territorial organization of direction-selective ganglion cells in rabbit retina. J Neurosci 14:6301–6316.

Wässle H, Boycott BB. 1991. Functional architecture of the mammalian retina. Physiol Rev 71:447–480.

Wässle H, Levick WR, Cleland BG. 1975. The distribution of the alpha type of ganglion cells in the cat's retina. J Comp Neurol 159:419–438.

Wässle H, Peichl L, Boycott BB. 1981. Morphology and topography of on- and off-alpha cells in the cat retina. Proc R Soc Lond B Biol Sci 212:157–175.

Wässle H, Voigt T, Patel B. 1987. Morphological and immunocytochemical identification of indoleamine-accumulating neurons in the cat retina. J Neurosci 7:1574–1585.

Watanabe M, Rodieck RW. 1989. Parasol and midget ganglion cells of the primate retina. J Comp Neurol 289:434–454.

Watanabe M, Fukuda Y, Hsiao C-F, Ito H. 1985. Electron microscopic analysis of amacrine and bipolar cell inputs on Y-, X- and W-cells in the cat retina. Brain Res 358:229–240.

Weber AJ, McCall MA, Stanford LR 1991. Synaptic inputs to physiologically identified retinal X-cells in the cat. J Comp Neurol 314:350–366.

Williams RW, Bastiani MJ, Chalupa LM. 1983. Loss of axons in the cat optic nerve following fetal enucleation: an electron microscopic analysis. J Neurosci 3:133–144.

Wingate JT, Fitzgibbon T, Thompson ID. 1992. Lucifer Yellow, retrograde tracers, and fractal analysis characterise adult ferret retinal ganglion cells. J Comp Neurol 323:449–474.

Wong ROL, Hughes A. 1987. The morphology, number, and distribution of a large population of confirmed displaced amacrine cells in the adult cat retina. J Comp Neurol 255:159–177.